

1 A useful technique using imaging mass spectrometry for detecting the skin distribution  
2 of topically applied lidocaine

3

4 Shosho Kijima<sup>a</sup>, Hiroaki Todo<sup>a</sup>, Yumi Matsumoto<sup>c</sup>, Ryosuke Masaki<sup>a</sup>, Wesam R.  
5 Kadhum<sup>a</sup>, Kenji Sugibayashi<sup>a,b\*</sup>

6

7 <sup>a</sup>Faculty of Pharmaceutical Sciences and <sup>b</sup>Life Science Research Center, Josai  
8 University, 1-1 Keyakidai, Sakado, Saitama 350-0295, Japan

9 <sup>c</sup>Global Application Development Center, Analytical & Measuring Instruments Division,  
10 Shimadzu Corporation, 1 Nishinokyo, Kuwabara-cho, Nakagyo-ku, Kyoto 604-8511,  
11 Japan

12

13 -----

14 \*To whom correspondence should be addressed:

15 Kenji Sugibayashi, Ph.D.

16 Faculty of Pharmaceutical Sciences, Josai University

17 1-1 Keyakidai, Sakado, Saitama 350-0295, Japan

18 Tel.: 049-271-7943

19 Fax: 049-271-8137

20 E-mail: [sugib@josai.ac.jp](mailto:sugib@josai.ac.jp)

21

22

1 Abstract

2 The skin disposition of topically applied lidocaine hydrochloride was determined  
3 under steady-state skin permeation by imaging mass spectrometry (MSI). The  
4 distribution of lidocaine in pig ear skin was assessed using MALDI-TOF-MS with mass  
5 images being examined with BioMap software. Following the detection of intrinsic  
6 signals of lidocaine, the skin concentration-distance curve was obtained using  
7 brightness analysis ( $[M+H]^+$ ;  $m/z$  235.18). Although the skin concentration profile  
8 obtained by MALDI-TOF-MS did not completely correspond to the calculated one  
9 obtained from the skin permeation profile, the skin concentration profile could be  
10 detected. These results demonstrate that imaging MSI might be a useful method that  
11 can be used to determine the skin disposition of topically applied non-radiolabeled or  
12 non-fluorescent drugs.

13

14 Keywords: imaging mass spectrometry; transdermal delivery; topical application; skin  
15 concentration; skin distribution

16

17

18

## 1 1. Introduction

2       The skin disposition of topically applied drugs is known to be strongly associated  
3 with local efficacy and toxicity (Holford et al., 1981). Dermatopharmacokinetics  
4 (Alberti et al., 2001) (DPK) is now being utilized to evaluate generic topical  
5 formulations in Japan ([www.nihs.go.jp/drug/be-guide\(e\)/Topical\\_BE-E.pdf](http://www.nihs.go.jp/drug/be-guide(e)/Topical_BE-E.pdf)). The skin  
6 concentrations of topically applied drugs have previously been assessed using several  
7 methods, including tape stripping (Pershing et al., 1992; N'Dri-Stempfer et al., 2009),  
8 heat separation (Surber et al., 1990), and others (Kiistala, 1968; Surber et al., 1993),  
9 which generally require drug extraction and tissue homogenization procedures.  
10 However, difficulties have been reported in accurately determining the drug distribution  
11 or drug concentration-distance profiles in the skin by these methods. The skin  
12 permeation profiles of topically applied drugs can be analyzed by Fick's second law of  
13 diffusion under the assumption that the skin consists of one or two homogeneous  
14 membranes (Sugibayashi et al., 2010). We recently reported that the skin  
15 concentrations of topically applied drugs in a certain logarithmic range of the  
16 *n*-octanol/water coefficient,  $\log K_{o/w}$  ( $1.93 < \log K_{o/w} < 2.81$ ), could be calculated with a  
17 two-layered diffusion model, with a relationship being identified between the calculated  
18 and observed steady-state concentrations of drugs. On the other hand, the skin  
19 concentrations of hydrophilic drugs ( $\log K_{o/w} \leq 0$ ) could not be accurately determined  
20 using the same method. Several studies (Lademann et al., 1999; Toll et al., 2004;  
21 Trauer et al., 2009; Marshall et al., 2010) confirmed that hair follicles and sweat ducts  
22 were the primary permeation pathways for hydrophilic drugs and macromolecules.

1 Fluorescence dyes such as calcein, fluorescein, and fluorescein isothiocyanate dextran  
2 (FITC-dextran) have been used as model hydrophilic drugs and macromolecules in  
3 order to provide insight into their skin disposition following topical application.  
4 However, this technique can only be used for fluorescent compounds.

5 Recently, several studies have used mass spectrometry imaging (MSI) by  
6 matrix-assisted laser desorption/ionization (MALDI) to investigate the disposition of a  
7 drug after its topical application (Marshall et al., 2010; Enthaler et al., 2011). In  
8 addition, D'Alvise et al. have reported that the follicular transport of lidocaine in the  
9 deeper skin layers and its metabolism in subcutaneous tissue could be detected by  
10 desorption electrospray ionization mass spectrometry imaging (D'Alvise et al., 2014).

11 The observation of heterogeneous drug distribution in skin, such as localized drug  
12 distributions in hair follicles, using a horizontal or vertical skin section with a  
13 microscope would provide us with very useful information to reveal the skin permeation  
14 route of topically applied drugs. Since the pharmacological and toxicological effects  
15 of topically applied chemicals can be determined by their concentration at the viable  
16 epidermis/dermis, drug concentration-depth profile in viable epidermis/dermis should  
17 be investigated in order to evaluate the safety and effects. Bunch et al. have reported  
18 that a quantitative skin profile of ketoconazole was acquired with MALDI quadrupole  
19 time-of-flight mass spectrometry (Q-TOFMS) (Bunch et al., 2004). However, no  
20 comparison of skin concentration profiles obtained by imaging MALDI-TOF MS and a  
21 conventional method has been performed to investigate the usefulness of the novel  
22 method.

1 In the present study, an atmospheric-pressure MALDI quadrupole-ion-trap TOF-MS  
2 (AP-MALDI-QIT-TOF-MS) instrument was first used with 10- $\mu$ m spatial resolution to  
3 obtain positional information on the concentration of a drug in skin following its topical  
4 application. Lidocaine hydrochloride was used as a model drug to observe the drug  
5 concentration-distance profile by MALDI-TOFS because its skin permeation profile  
6 could be successfully calculated with Fick's second law of diffusion from the skin  
7 permeation profile.

8

## 9 2. Experimental

### 10 2.1. Materials and methods

11 Lidocaine hydrochloride was obtained as a model drug from Sigma Aldrich (St.  
12 Louis, MO, U.S.A.). Other reagents and solvents were of reagent or HPLC grade and  
13 used without further purification. Frozen pig ear skin (three-breed cross pigs involving  
14 the Landrace, Yorkshire and Durocbreeds) was purchased from the National Federation  
15 of Agricultural Cooperative Associations (Tokyo, Japan). The skin samples were  
16 stored at -30°C until the skin permeation experiments.

17

### 18 2.2. Preparation of skin membrane

19 The purchased skin was maintained frozen at -80°C prior to use. The skin was  
20 thawed at 32°C and excised from the outer surface of a pig ear after being cleaned with  
21 distilled water. Stripped skin was obtained by tape stripping of the stratum corneum

1 (SC) with adhesive tape (Scotch<sup>®</sup>; 3M Japan Ltd., Tokyo, Japan) 20 times prior to its  
2 excision from the pig ear. Excess fat was carefully trimmed off from the excised skin  
3 with a knife.

4

### 5 2.3. Skin permeation experiments for lidocaine

6 The skin sample was set in a vertical-type diffusion cell (effective diffusion area: 1.77  
7 cm<sup>2</sup>) in which the skin surface temperature was maintained at 32°C. After 1 h of  
8 hydration with phosphate-buffered solution (PB), PB containing 2.5 mg/mL lidocaine  
9 (volume: 1.0 mL) was applied to the SC side as a donor solution for 8 h, and PS  
10 (volume: 6.0 mL) was added to the dermis side as a receiver solution. The receiver  
11 solution was stirred with a stirrer bar on a magnetic stirrer. An aliquot (500 µL) was  
12 withdrawn from the receiver chamber and the same volume of PB was added to the  
13 chamber to keep the volume constant. The penetrant concentration in the receiver  
14 chamber was determined by HPLC. Three skin permeation experiments were  
15 conducted to calculate the skin concentration-distance profile.

16

### 17 2.4. HPLC conditions

18 Ethyl paraben (EB) was used as an internal standard (IS) in the quantitative  
19 determination of lidocaine. An aliquot of a sample solution containing lidocaine was  
20 mixed with acetonitrile (1:1) and centrifuged (15,000 × rpm, 5 min, 4°C) to obtain  
21 supernatant. Then, 20 µL of obtained supernatant was injected into the HPLC system.  
22 The HPLC system consists of a pump (LC-20AD), a UV detector (PD-20A), a

1 system controller (SCL-10A<sup>VP</sup>), an auto-injector (SIL-20A), a degasser  
2 (DGU-20A<sub>3</sub>), a column oven (CTO-20A), and analysis software (LC solution)  
3 (all from Shimadzu, Kyoto, Japan). An Inertsil- ODS-3 5 μm, 4.6×150 mm  
4 (GL Sciences Inc., Tokyo, Japan) column was kept at 40°C. The mobile  
5 phase was 0.1% phosphoric acid:acetonitrile = 7:3, containing 5.0 mM  
6 1-heptanesulfonate at a flow rate of 1.0 ml/mL. Detection was carried out  
7 at UV 230 nm.

8

#### 9 2.5. Preparation of skin samples to plot lidocaine calibration curve

10 The stripped skin was immersed in different concentrations of lidocaine solution (500,  
11 1500, and 2500 μg/mL) for 24 h to obtain skin with homogeneously distributed  
12 lidocaine. A calibration curve for the skin concentration of lidocaine was obtained by  
13 imaging analysis of the treated skin.

14

#### 15 2.6. Skin treatment for MALDI-TOFS observation

16 After the permeation experiment or after immersion in lidocaine solutions to obtain  
17 a calibration curve, the skin surface was washed three times using 1 mL of ultrapure  
18 water. The skin was then embedded in 2.0% carboxymethyl cellulose and frozen in  
19 isopentane at -80°C. The embedded skin was sliced using a cryostat (CM3050; Leica  
20 Microsystems, Wetzler, Germany) to obtain 7-μm-thick vertical sections at -20°C.  
21 Then, each skin section was kept at room temperature for 30 min before subjecting it to  
22 MALDI-QIT-TOF-MS. These sections were mounted on an indium tin oxide-coated

1 slide glass (Sigma-Aldrich), dried in a silica gel-containing plastic tube, and then  
2 sprayed with 2,5-dihydroxybenzoic acid (DHB; 50 mg/mL in 70% methanol and 30%  
3 water containing trifluoroacetic acid at a concentration of 0.1%) using a 0.2-mm-nozzle  
4 caliber airbrush (Procon Boy FWA Platinum; Mr. Hobby, Tokyo, Japan) to conduct  
5 MALDI-imaging mass spectrometry in the positive-ion mode. MALDI-QIT-TOF-MS  
6 equipped with a 355-nm Nd:YAG laser and microscope allowed mass images to be  
7 obtained with a high spatial resolution of 10  $\mu\text{m}$ , in the scan range of  $m/z$  200-900, as  
8 described previously for a prototype MALDI-imaging mass spectrometry instrument  
9 (Marshall et al., 2010) (Mass Microscope; Shimadzu, Kyoto, Japan). Microscopic  
10 images were obtained after application of a matrix (300  $\mu\text{L}$  of DHB solution) to the skin  
11 sections. Mass spectra were subsequently acquired in the positive-ion mode in the  
12 designated areas of a specimen.

13

#### 14 2.7. Image analysis of skin sections using BioMap<sup>®</sup>

15 The distribution of the specific signal intensity of lidocaine ( $[M+H]^+$ :  $m/z$  235.18)  
16 in the skin was assessed using AP-MALDI-TOF-MS with mass images being examined  
17 with BioMap<sup>®</sup> software (Novartis Pharma K.K., Basel, Switzerland). The brightness of  
18 the obtained skin section images was analyzed using the image processing software  
19 Image J<sup>®</sup> (National Institutes of Health, Bethesda, MD, U.S.A.). Figure 1a shows  
20 microscopic observation results of a skin section. The measurement area in the skin  
21 section was decided by the positional information of the obtained image and the area,  
22 and was then divided into 5 sections (the size of each section: 260  $\mu\text{m}$  long  $\times$  500  $\mu\text{m}$

1 wide) from the surface of stratum corneum side ( $x = 0$ ) to calculate the brightness  
2 intensity (Figure 3b). The average brightness value in each section was obtained using  
3 Image J software (ver. 1.48). In the case of the full-thickness skin to measure the skin  
4 concentration of lidocaine, the outermost section to the stratum corneum side was  
5 further divided into two sections; the size of the outermost section was  $20 \mu\text{m}$  long  $\times$   
6  $500 \mu\text{m}$  wide and that of the other one was  $240 \mu\text{m}$  long  $\times$   $500 \mu\text{m}$  wide.

7

## 8 2.8. Calculation of skin concentration from skin permeation profile

9 The calculated skin concentration of lidocaine was obtained by curve-fitting the  
10 cumulative amount of it that permeated through the full-thickness skin and stripped skin  
11 to the theoretical values, where the theoretical values could be expressed by Fick's  
12 second law of diffusion in the stratum corneum and viable epidermis and dermis.  
13 Differential equations describing Fick's second law are as follows.

$$14 \quad \frac{dC_{i,j+1}}{dt} = \frac{1}{\Delta t} (C_{i,j+1} - C_{i,j}) \quad (1)$$

$$15 \quad \frac{dC_{i,j}}{dx^2} = \frac{1}{\Delta x^2} (C_{i-1,j} - 2C_{i,j} + C_{i+1,j}) \quad (2)$$

16 The mathematical approach for determining skin permeation using a two-layered  
17 diffusion model was the same as in our previous method (Sugibayashi et al., 2010).  
18 Skin permeation parameters such as permeability coefficient, diffusion coefficient, and  
19 partition coefficient were obtained by curve-fitting to the obtained permeation profiles  
20 with a two-layered diffusion model.

21

1

## 2 2.9. Measurement of skin thickness

3 The thicknesses of the stratum corneum, epidermis, and whole skin in pig ear skin was  
4 microscopically determined from microtomed sections after hematoxylin–eosin staining.  
5 Five section selected at random from each specimen were used to measure the stratum  
6 corneum, and whole skin thicknesses were measured by a light micrograph (IX71;  
7 Olympus Corp., Tokyo, Japan) and a calibrated ocular micrometer. The thickness of the  
8 epidermis was calculated by subtracting the stratum corneum thickness from the whole  
9 skin thickness.

10

## 11 3. Results

### 12 3.1. Skin permeation profile of lidocaine

13 Figure 1 shows the skin permeation profiles of lidocaine through full-thickness skin  
14 and stripped skin after its topical application. The cumulative amount of lidocaine that  
15 permeated through the stripped skin was much higher than that through the  
16 full-thickness skin. Skin permeation parameters obtained from the permeation profiles  
17 through the full-thickness and stripped skin are listed in Table 1. Since the skin  
18 thickness of stratum corneum and viable epidermis and dermis were  $19.0 \pm 2.0 \mu\text{m}$   
19 (mean  $\pm$  S.E.) and  $1406 \pm 38 \mu\text{m}$  (mean  $\pm$  S.E.), these values were set to calculate the  
20 skin permeation parameters. The skin concentration-distance profiles in full-thickness  
21 and stripped skin that were calculated with the skin permeation parameters are shown in  
22 Figures 6a and b, respectively. The ratio of lidocaine concentration at depth 0 to the

1 distance from the stratum corneum was much higher than that at other distance points,  
2 and the lidocaine concentration in the skin gradually decreased toward the dermis side  
3 from the stratum corneum.

4  
5 Fig. 1

### 6 7 3.2. Fractionation of lidocaine signals by MSI

8 Figure 2 shows a typical mass spectrum, collected from  $m/z=200$  to  $900$ , of a skin  
9 section after the topical application of lidocaine. The mass peak of protonated  
10 lidocaine was present ( $m/z$  235.18) in the skin section.

11  
12 Fig. 2

### 13 14 3.3. MSI observations of pig ear skin sections and image analysis using BioMap<sup>®</sup>

15 Figure 3a shows optical images of a skin section after the skin had been immersed  
16 in lidocaine solution at a concentration of  $1500 \mu\text{g/mL}$  in order to obtain a calibration  
17 curve. The distribution of lidocaine was determined in a designated square area of the  
18 skin that is enclosed by black lines in Fig. 3a. Figure 3b shows the distribution of  
19 lidocaine, which could be identified by MS analysis and visualized as mass images with  
20 BioMap software. The skin distribution of lidocaine is shown as a red spot. The  
21  $[\text{M}+\text{H}^+]$  signal was detected in the whole area of the skin.

1 Figs. 3a and 3b

2

### 3 3.4. Imaging analysis of lidocaine in skin sections using Image J software

4 To evaluate the skin distribution of lidocaine, the distribution of signals was  
5 quantified based on the depth direction using Image J software. Figures 4a and b show  
6 optical images of a skin section and the lidocaine distribution in the stripped skin after  
7 immersion in solutions with different concentrations of lidocaine (0, 500, 1500, and  
8 2500  $\mu\text{g}/\text{mL}$ ), respectively. Lidocaine distributions were observed in each skin sample,  
9 and the brightness of red spots increased with an increase of the applied concentration  
10 of lidocaine. Figure 4c shows the correlation between brightness intensity and skin  
11 concentration of lidocaine. A good relationship ( $R^2=0.998$ ) was observed within the  
12 range of lidocaine concentrations up to 2500  $\mu\text{g}/\text{mL}$ .

13

14 Figures 4a, 4b, and 4c

15

16 Figures 5 and 6 show lidocaine distribution and its concentration-depth profiles in the  
17 stripped skin and the viable epidermis and dermis parts of full-thickness skin. The  
18 lidocaine distributions were detected in both stripped skin and full-thickness skin and  
19 many bright dots were confirmed in stripped skin compared with those in full-thickness  
20 skin. The obtained skin concentrations from MSI analysis were corrected with  $K_{\text{ved}}$   
21 value of lidocaine and the observed skin concentrations was plotted against the average  
22 value of the depth of each skin section. As shown in Fig. 6, calculated lidocaine

1 concentration in skin was decreased in the stripped skin as well as in the full-thickness  
2 skin toward the dermis from the stratum corneum side. The observed lidocaine  
3 concentration in stripped skin was lower than calculated one, whereas the observed  
4 concentration in full-thickness skin was higher than calculated one. Although the  
5 profiles did not correspond to each other, skin concentration-depth profiles obtained  
6 from MSI analysis showed almost the same tendencies as the calculated ones.

7

8

Fig. 5

9

#### 10 4. Discussion

11 The DPK test in the stratum corneum for topically applied drugs by the tape-stripping  
12 method would be helpful for evaluating the bioequivalence of topically applied drugs  
13 (Kalia et al., 2000). Although LC/MS, LC/MS/MS and accelerator mass spectrometry  
14 are a sensitive technique to detect drug concentration, these are limitations for detecting  
15 its disposition in a tissue correctly. It is an evidence that Hill equation could be  
16 applied to reveal the relationship between pharmacodynamics or toxicodynamics of  
17 drugs and its tissue concentration. Therefore, establishment of drug disposition in skin  
18 with an imaging analysis would be very useful for evaluation of safety and effects of  
19 topically applied chemicals. In our previous experiment (Kijima et al., 2015), a  
20 non-steady state of drug concentration-skin depth profile could be detected by confocal  
21 laser scanning microscopy after the application of a fluorescent marker, and DPK  
22 parameters could be calculated with Fick's second law of diffusion. Therefore, in the

1 present experiment, the skin concentration-depth profile of topically applied  
2 non-labeled drug was investigated to confirm the possibility of DPK analysis with MSI  
3 analysis.

4 A calibration curve to detect the lidocaine concentration in the skin was achieved with  
5 the combination of MSI observation and imaging analysis using Image J software. In  
6 the present experiment, calibration curve was obtained from immersed skin in different  
7 concentrations of lidocaine solution. Skin concentration of lidocaine was corrected  
8 with the  $K_{ved}$  value that obtained from *in vitro* skin permeation profile through stripped  
9 skin. Therefore, when another chemical was selected, the skin concentrations to  
10 calculate skin concentration curve could be corrected with its partition coefficient value.

11 Oshizaka et al (2014) reported that skin concentration could be calculated using a skin  
12 resistance model. Skin permeation resistance in stratum corneum ( $R_{sc}$ ), which is equal  
13 to the reciprocal value of the drug permeation coefficient through the stratum corneum  
14 ( $1/P_{sc}$ ), could be calculated by subtraction of the reciprocal value of the skin permeation  
15 coefficient through full-thickness skin ( $1/P_{tot}$ ) to that through stripped skin ( $1/P_{ved}$ )  
16 (Scheuplien et al., 1971). A high  $R_{sc}$  value provides a high drug concentration gradient  
17 across the stratum corneum.  $R_{sc}$  of lidocaine showed about 90% of total skin resistance  
18 and the remaining 10% was  $R_{ved}$  in the present study. Thus, lidocaine concentration  
19 would be dramatically decreased across the stratum corneum in Fig. 6b. In our  
20 previous study, the lidocaine concentration-distance profile obtained from the skin  
21 permeation profile corresponded well to the observed one (Oshizaka et al., 2014).  
22 Lidocaine concentration-distance profiles obtained from MSI analysis in the stripped

1 and full-thickness skin differed from the calculated values. However, these measured  
2 values obtained from MSI analysis were relatively close to the calculated ones. Thus,  
3 this method would be applicable for the detection of drug concentration in skin. When  
4 stripped skin was analyzed with MSI, the observed skin concentrations were lower than  
5 calculated values. On the other hand, the observed concentrations in the full-thickness  
6 skin was higher than the calculated ones. These results might be related to lidocaine  
7 diffusion in the skin from high to low concentrations during matrix coverage process  
8 before measurement of lidocaine with MALDI-TOF-MS. Thus, LC concentration in  
9 stripped skin might be decreased by the diffusion from the inside to the outside of the  
10 skin and the concentration in the full-thickness skin might be increased by the diffusion  
11 from the stratum corneum to the viable epidermis and dermis compared with calculated  
12 values.

13 In our previous study (Kijima et al., 2015), drug concentration-depth profiles obtained  
14 from imaging analysis by confocal laser-scanning microscopy at non-steady-state and  
15 steady-state conditions corresponded fairly well with those obtained from the skin  
16 permeation experiments. The measurement by laser-scanning microscopy was  
17 conducted without a pretreatment procedure. Thus, improvement of procedure might  
18 be necessary to analyze drug concentration correctly with MSI analysis.

19 Bunch et al. (2004), Sjövall et al. (2014), Judd et al. (2013), and D'Alvise (2014)  
20 have investigated the drug distribution in skin using MSI analysis. In addition, many  
21 reports have been published on the usefulness of MSI analysis as a potential tool for  
22 measurement of the distribution of compounds in tissues (Buck et al., 2015; Hamm et

1 al., 2012; Grobe et al., 2012). Internal standard was not used to conduct the MSI  
2 analysis for detection of lidocaine disposition in the skin in the present study. To  
3 compensate for variation of the acquired brightness of red spots images, the average  
4 value of brightness was used in the divided skin sections. Although drug-disposition  
5 profiles in the full thickness skin was achieved by skin-thickness information obtained  
6 from the optical image and the profiles were relatively close to the calculated ones with  
7 two-layered model, this approach would be not suitable for detection of drug  
8 concentration in specific area such as hair follicles, sweat ducts and interfacial layers  
9 between different cells. Furthermore, skin is histologically composed of three layers  
10 and the line of these layers are not straight, but markedly wavy. Thus, measurement of  
11 drug skin with divided skin section area might be difficult to measure its concentration  
12 in each layer of the skin. The use of an internal standard to perform quantitative  
13 analysis should be needed with MSI analysis in the further experiment to analyze more  
14 detail drug distribution in the skin.

15 Judd et al (2013) have investigated the detection of drug disposition in the stratum  
16 corneum with ToF-SIMS by the combination of tape-stripping method. Although  
17 high-sensitive analysis was successfully conducted with this combination approach,  
18 drug concentration in viable epidermis and dermis could not be measured with this  
19 approach. Few studies have reported that a comparison of topically applied drug  
20 concentrations measured by MSI analysis and conventional techniques such as  
21 extraction and tissue homogenization procedures. Thus, the present work showed the  
22 usefulness of MSI analysis technique to evaluate drug disposition and concentration in

1 skin after its topical application. This approach would be complementary method to  
2 evaluation of skin permeation of drugs with conventional diffusion cells.

3

#### 4 5. Conclusion

5 Investigation of the dermatopharmacokinetics (DPK) should be performed to  
6 develop topical formulations and drug formulas. In the present study, only the  
7 lidocaine distribution in skin was evaluated. To clarify the usefulness of this approach,  
8 the skin distribution of compounds with a wide range of physicochemical properties  
9 should be investigated. Although further experiments involving DPK analysis with the  
10 obtained data are required, this result suggests that the drug concentration profile in  
11 viable epidermis and dermis could be obtained, and evaluations of the safety and effect  
12 of chemicals as well as evaluation of their disposition in the skin might be conducted by  
13 observation using MSI.

14

15

1 References

- 2 Albert, I., Kalia, Y.N., Naik, A. and Guy, R.H., 2001. Assessment and prediction of the  
3 cutaneous bioavailability of topical terbinafine, in vivo, in man. *Pharm. Res.*, 18,  
4 1472-1475.
- 5 Bunch, J., Clench, M.R., Richards, D.S., 2004. Determination of pharmaceutical  
6 compounds in skin by imaging matrix-assisted laser desorption/ionisation mass  
7 spectrometry. *Rapid Commun. Mass Spectrom.*, 18, 3051–3060.
- 8 Buck, A., Halbritter, S., Späth, C., Feuchtinger, A., Aichler, M., Zitzelsberger, H.,  
9 Janssen, K.-P., Walch, A., 2015. Distribution and quantification of irinotecan and its  
10 active metabolite SN-38 in colon cancer murine model systems using MALDI MSI.  
11 *Anal. Bioanal. Chem.*, 407, 2107–2116.
- 12 Enthaler, B., Pruns, J. K., Wessel, S., Rapp, C., Fischer, M., & Wittern, K.-P., 2011.  
13 Improved sample preparation for MALDI–MSI of endogenous compounds in skin  
14 tissue sections and mapping of exogenous active compounds subsequent to ex-vivo skin  
15 penetration. *Analytical and Bioanalytical Chemistry*, 402, 1159–1167.
- 16 D’Alvise, J., Mortensen, R., Hansen, S. H., & Janfelt, C., 2014. Detection of follicular  
17 transport of lidocaine and metabolism in adipose tissue in pig ear skin by DESI mass  
18 spectrometry imaging. *Analytical and Bioanalytical Chemistry*, 406, 3735–3742.
- 19 Grobe, N., Elased, K.M., Cool, D.R., Morris, M., 2012. Mass spectrometry for the  
20 molecular imaging of angiotensin metabolism in kidney. *Am. J. Physiol. Endocrinol.*  
21 *Metab.*, 302, E1016–E1024.
- 22 Hamm, G., Bonnel, D., Legouffe, R., Pamelard, F., Delbos, J.-M., Bouzom, F., Stauber,

1 J., 2012. Quantitative mass spectrometry imaging of propranolol and olanzapine using  
2 tissue extinction calculation as normalization factor. *J. Proteomics.*, 75, 4952–4961.

3 Holford N.H., Sheiner L.B., 1981. Understanding the dose-effect relationship: clinical  
4 application of pharmacokinetic-pharmacodynamic models. *Clin. Pharmacokinet.*, 6,  
5 429-453.

6 Judd, A.M., Scurr, D.J., Heylings, J.R., Wan, K.-W., Moss, G.P., 2013. Distribution and  
7 Visualisation of Chlorhexidine Within the Skin Using ToF-SIMS: A Potential Platform  
8 for the Design of More Efficacious Skin Antiseptic Formulations. *Pharm Res* 30, 1896–  
9 1905.

10 Kalia, Y. N., Alberti, I., Sekkat, N., Curdy, C., Naik, A., & Guy, R. H., 2000.  
11 Normalization of stratum corneum barrier function and transepidermal water loss in  
12 vivo. *Pharmaceutical Research*, 17, 1148–1150.

13 Kiistala U., 1968. Suction blister device for separation of viable epidermis from dermis.  
14 *J. Invest. Dermatol.*, 50, 129-137.

15 Kijima S., Masaki R., Kadhum W.R., Todo H., Hatanaka T., Sugibayahi K., 2015.  
16 Potential of imaging analysis in establishing skin concentration-distance profiles for  
17 topically applied FITC-dextran 4 kDa. *ADMET & DMPK.*, 2, 221–234.

18 Kubo, A., Ohmura, M., Wakui, M., Harada, T., Kajihara, S., Ogawa, K., et al. (2011).  
19 Semi-quantitative analyses of metabolic systems of human colon cancer metastatic  
20 xenografts in livers of superimmunodeficient NOG mice. *Analytical and Bioanalytical*  
21 *Chemistry*, 2011; 400: 1895–1904.

22 Lademann J., Weigmann H., Rickmeyer C., Barthelmes H., Schaefer H., Mueller G.,

1 Sterry W., 1999. Penetration of titanium dioxide microparticles in a sunscreen  
2 formulation into the horny layer and the follicular orifice. *Skin Pharmacol. Appl. Skin*  
3 *Physiol.*, 12, 247-256.

4 Marshall, P., Toteu-Djomte, V., Bareille, P., Perry, H., Brown, G., Baumert, M., &  
5 Biggadike, K., 2010. Correlation of Skin Blanching and Percutaneous Absorption for  
6 Glucocorticoid Receptor Agonists by Matrix-Assisted Laser Desorption Ionization  
7 Mass Spectrometry Imaging and Liquid Extraction Surface Analysis with  
8 Nanoelectrospray Ionization Mass Spectrometry. *Analytical Chemistry*, 82, 7787–7794.

9 N'Dri-Stempfer B., Navidi W.C., Guy R.H., Bunge A.L., 2009. Improved  
10 bioequivalence assessment of topical dermatological drug products using  
11 dermatopharmacokinetics. *Pharm. Res.*, 26, 316-328.

12 Oshizaka, T., Kikuchi, K., Kadhum, W.R., Todo, H., Hatanaka, T., Wierzba, K.,  
13 Sugibayashi, K., 2014. Estimation of skin concentrations of topically applied lidocaine  
14 at each depth profile. *Int. J. Pharm.*, 475, 292–297.

15 Pershing L.K., Silver B.S., Krueger G.G., Shah V.P., Skelley J.P., 1992. Feasibility of  
16 measuring the bioavailability of topical betamethasone dipropionate in commercial  
17 formulations using drug content in skin and a skin blanching bioassay. *Pharm. Res.*, 9,  
18 45-51.

19 Scheuplien, R.J., BLANK, I.H., 1971. Permeability of the skin. *Physiol. Rev.*, 51,  
20 702-747

21 Sjövall, P., Greve, T.M., Clausen, S.K., Moller, K., Eirefelt, S., Johansson, B., Nielsen,  
22 K.T., 2014. Imaging of Distribution of Topically Applied Drug Molecules in Mouse

1 Skin by Combination of Time-of-Flight Secondary Ion Mass Spectrometry and  
2 Scanning Electron Microscopy. *Anal. Chem.* 86, 3443–3452.

3 Sugibayashi K., Todo H., Oshizaka T., Owada Y., 2010. Mathematical model to predict  
4 skin concentration of drugs: toward utilization of silicone membrane to predict skin  
5 concentration of drugs as an animal testing alternative. *Pharm. Res.*, 27, 134-142.

6 Surber C., Wilhelm K.P., Hori M., Maibach H.I., Guy R.H., 1990. Optimization of  
7 topical therapy: partitioning of drugs into stratum corneum. *Pharm. Res.* 7, 1320–1324.

8 Surber C., Wilhelm K.P., Bermann D., Maibach H.I., 1993. In vivo skin penetration of  
9 acitretin in volunteers using three sampling techniques., *Pharm. Res.*, 10, 1291-1294.

10 Takeuchi H., Ishida M., Furuya A., Todo H., Urano H., Sugibayashi K., Influence of  
11 skin thickness on the *in vitro* permeabilities of drugs through Sprague-Dawley rat or  
12 Yucatan micropig skin, *Biol. Pharm. Bull.*, 2012; 32: 192-202.

13 Teichmann A., Jacobi U., Ossadnik M., Richter H., Koch S., Sterry W., Lademann J.,  
14 2005. Differential stripping: determination of the amount of topically applied substances  
15 penetrated into the hair follicles. *J. Invest. Dermatol.*, 125, 264-269.

16 Toll R., Jacobi U., Richter H., Lademann J., Schaefer H., Blume Peytavi U., 2004.  
17 Penetration profile of microspheres in follicular targeting of terminal hair follicles. *J.*  
18 *Invest. Dermatol.*, 123, 168-176.

19 Trauer S., Patzelt A., Otberg N., Knorr F., Rozycki C., Balizs G., Buttemeyer R.,  
20 Linscheid M., Liebsch M., Lademann J., 2009. Permeation of topically applied caffeine  
21 through human skin--a comparison of in vivo and in vitro data. *Br. J. Clin. Pharmacol.*,  
22 68, 181-186.

1 Figure captions

2 Figure 1 Skin permeation of lidocaine through full-thickness skin (●) and stripped  
3 skin (○). The mean ± S.E. (n=4).

4

5 Figure 2 Typical MALDI mass spectrum, which was collected from  $m/z=200$  to  $900$ ,  
6 in skin sections without a) and with b) topical application of lidocaine at a concentration  
7 of  $2500 \mu\text{g/ml}$ .

8

9 Figure 3 Example of an IMS observation image for lidocaine intensity in a  
10 full-thickness pig ear skin section after the permeation experiment. a) Optical image of  
11 a vertical skin section. b) MSI image observation of distribution of lidocaine in skin  
12 after its topical application. The skin section was decided by the positional information  
13 of the obtained image. Abbreviation: SC, stratum corneum.

14

15 Figure 4 Calibration curve between applied lidocaine concentration [(i)  $0 \mu\text{g/mL}$ , (ii)  
16  $500 \mu\text{g/mL}$ , (iii)  $1500 \mu\text{g/mL}$ , and (iv)  $2500 \mu\text{g/mL}$ ] and its brightness. a) Optical  
17 image of skin (the MSI observed area is enclosed with black lines). b) MSI  
18 observation image in skin. c) Calibration curve obtained from applied lidocaine  
19 concentration and its intensity. Each pixel was  $10 \mu\text{m}$  in width. Each point  
20 represents the mean ± S.E. (n=5).

21

22 Figure 5 The optical and MSI observations of lidocaine after its topical application to

1 stripped (a and c) and full-thickness skins (b and d). a) and b) are optical images of a  
2 skin section, whereas c) and d) are MSI images. Scale bar shows 100  $\mu\text{m}$ .  
3  
4 Figure 6 Lidocaine concentration-depth profile in a) stripped and b) full-thickness  
5 skin and c) enlargement of b) in terms of the scale of the y-axis. The value of abscissa  
6 ( $x/L$ ) calculated from the ratio, which obtained from the positional information.  $L$  is  
7 set to be 1300  $\mu\text{m}$  from the surface of the skin.  
8 Symbols: ●, lidocaine concentration calculated from skin permeation parameters; ○,  
9 concentration observed by MSI image analysis.  
10

Table 1 Permeation parameters obtained from the skin permeation profile of LC

| Drug | Skin permeation parameters     |  |
|------|--------------------------------|--|
| LC   | $P_{tot}$ (cm/s)               | $7.97 \times 10^{-7} \pm 8.8 \times 10^{-8}$ |
|      | $P_{ved}$ (cm/s)               | $6.37 \times 10^{-6} \pm 4.1 \times 10^{-7}$ |
|      | $D_{sc}$ (cm <sup>2</sup> /h)  | $8.5 \times 10^{-7}$                         |
|      | $D_{ved}$ (cm <sup>2</sup> /h) | $2.2 \times 10^{-3}$                         |
|      | $K_{sc}$                       | 9.5  |
|      | $K_{ved}$                      | 1.7  |

$P_{tot}$ : skin permeation coefficient through the full-thickness skin

$P_{ved}$ : skin permeation coefficient through the stripped skin

$D_{sc}$ : diffusion coefficient of drug in the stratum corneum

$D_{ved}$ : diffusion coefficient of drug in the viable epidermis/dermis

$K_{sc}$ : diffusion coefficient of drug in the stratum corneum

$K_{ved}$ : diffusion coefficient of drug in the stratum corneum

Thicknesses of the stratum corneum and viable epidermis/dermis were set to be 15  $\mu\text{m}$  and 1485  $\mu\text{m}$ , respectively.

1

2

3

4

Figure 1

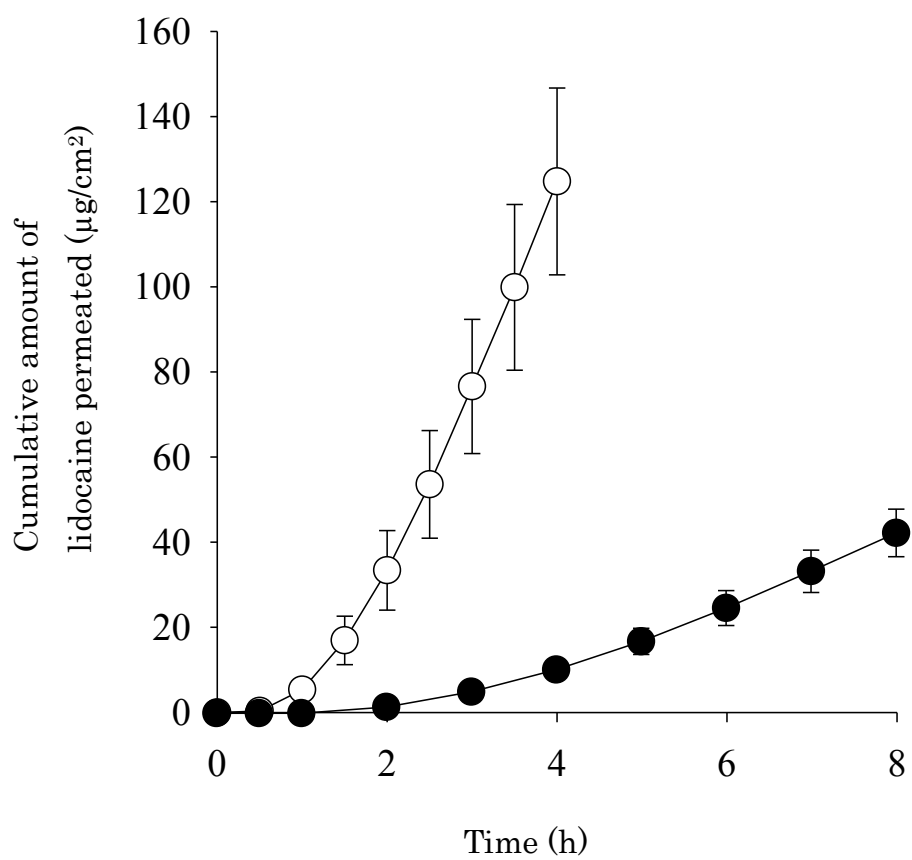
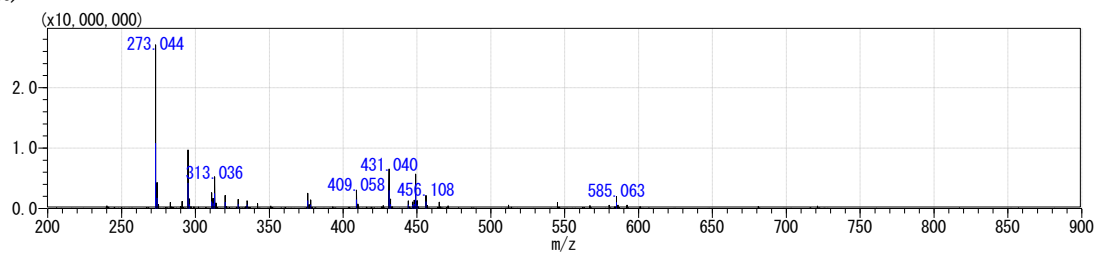


Figure 2

a)



b)

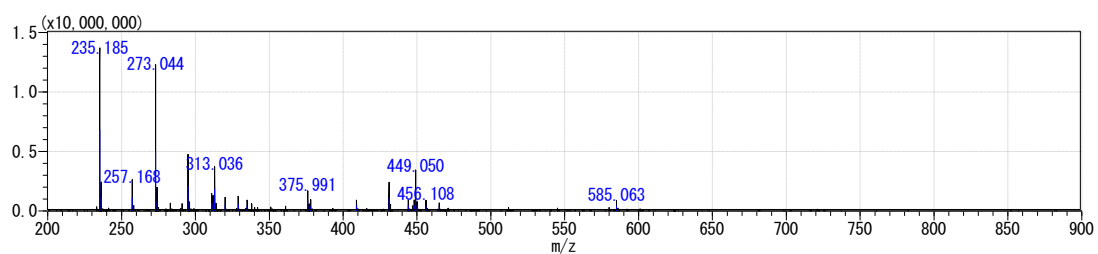


Figure 3

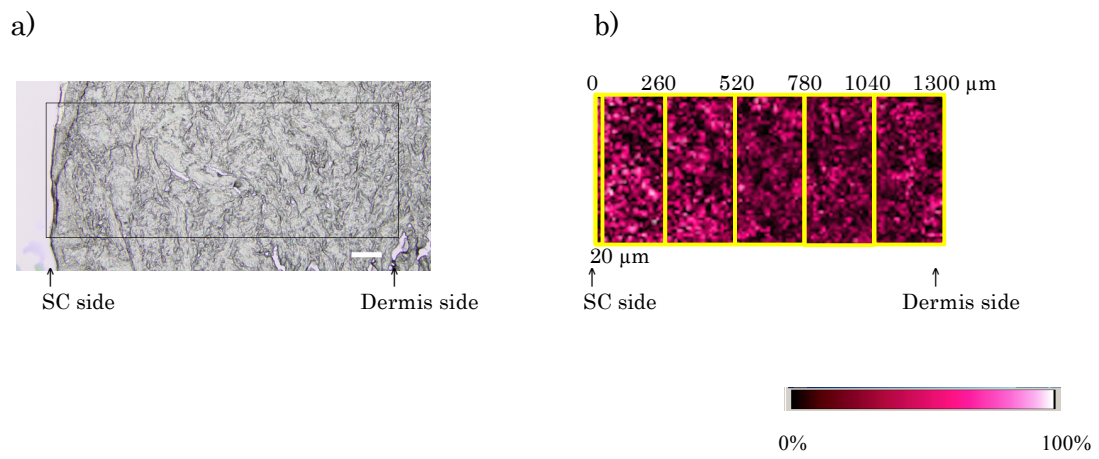


Figure 4

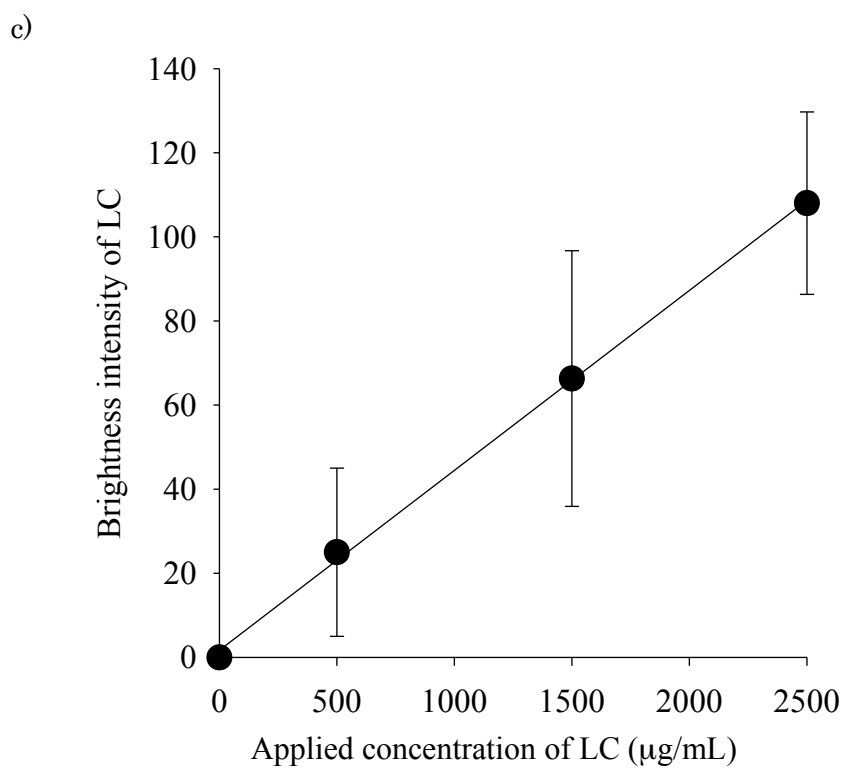
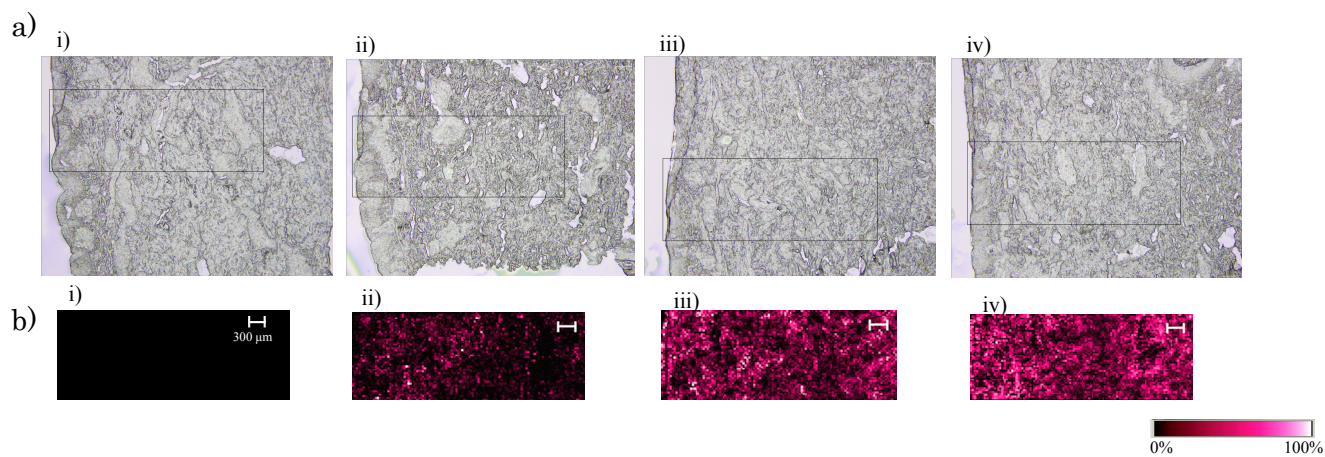


Figure 5

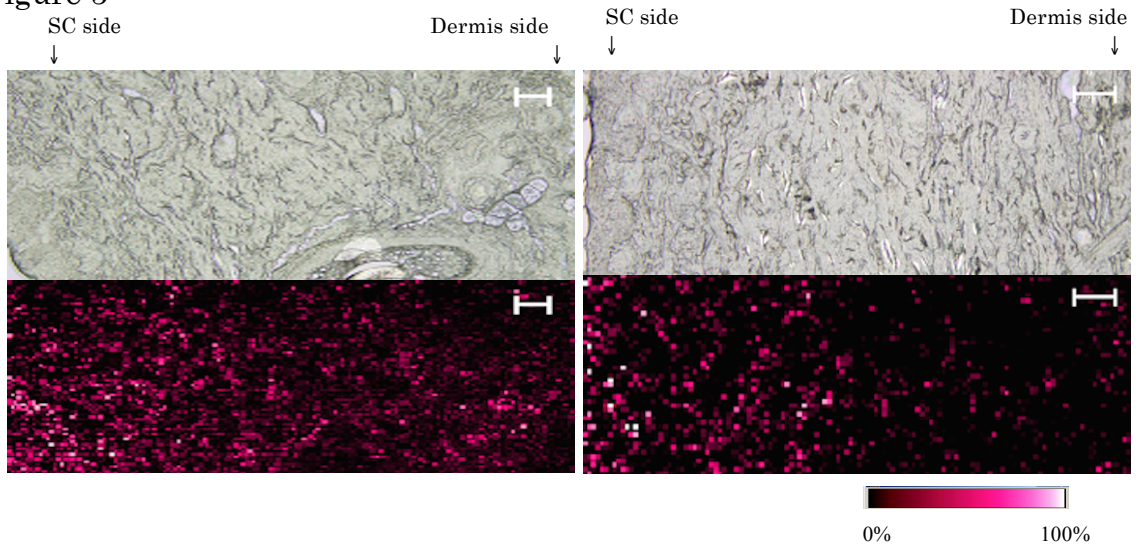
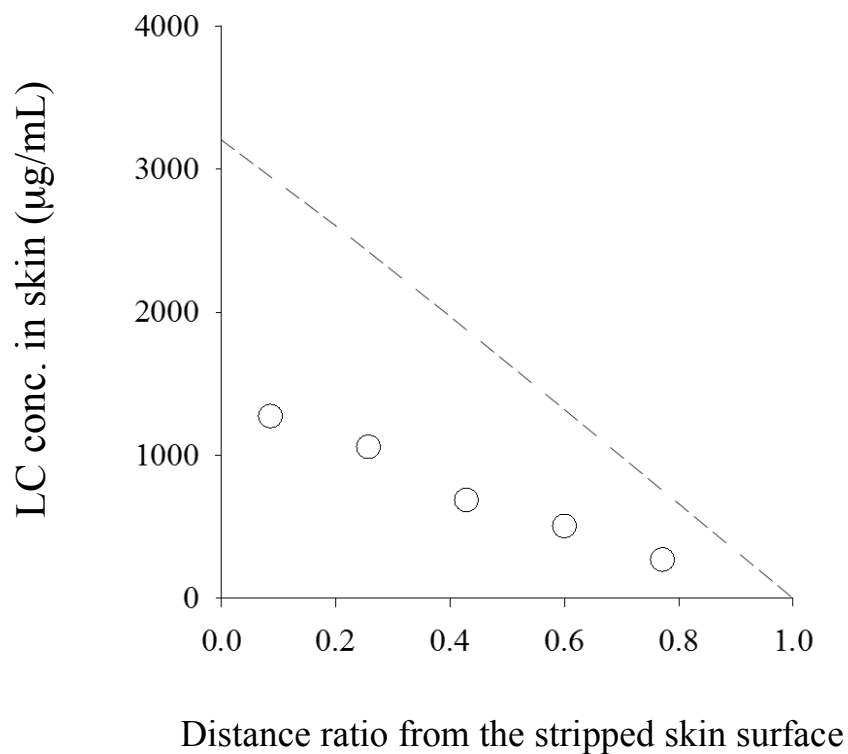


Figure 6

a)



b)

